arXiv:1404.2040v1 [cond-mat.str-el] 8 Apr 2014

Resonant inelastic x-ray scattering on single-magnons at oxygen K-edges

Beom Hyun Kim and Jeroen van den Brink
Institute for Theoretical Solid State State Physics,
IFW Dresden, Helmholtzstrasse 20, 01069 Dresden, Germany
(Dated: April 9, 2014)

The recent discovery that resonant inelastic x-ray scattering can probe single-magnon (SM) dispersions in transition metal (TM) oxides when the x-ray energy is tuned to the TM L-edge, has put this technique on a par with inelastic neutron scattering. It is generally presumed that selection rules forbid SM-scattering at oxygen (O) K-edges. However, based on a symmetry analysis and exact diagonalization study, we show that SM-scattering at O K-edges becomes allowed when (*i*) spin-orbit coupling is present in the TM d-shell and (*ii*) inversion symmetry at the O-site is broken. For cuprates the resulting SM-amplitude is very weak but in iridates both prerequisites can amply be fulfilled.

PACS numbers: 75.30.Ds,78.70.Ck,71.70.Ej

Introduction — The theoretical prediction [1] and subsequent experimental observation [2, 3] that the dispersion of magnetic excitations, in particular of elementary single-magnons, can be measured directly by resonant inelastic x-ray scattering (RIXS) has fundamentally changed the field of inelastic magnetic scattering [4]. It has for instance lead to the discovery of distinct paramagnons in a large family of high-temperature cuprate superconductors [3–8], and established the presence of strongly dispersive magnetic modes in a number of iridium oxides [9–12].

All these efforts to extract the dispersion of elementary magnetic excitations from RIXS have focussed on the transition metal (TM) L-edge, where single spin-flip scattering is directly allowed [1–16]. The microscopic origin of this type of magnetic scattering is rather straightforward. When energy in RIXS the incoming photon is tuned to a TM L-edge, an electron with spin σ is excited out of the atomic p-shell, deep inside the atomic core, into the TM d-shell. The core-hole that is created in this event can now flip its spin due its very large spin-orbit interaction. Subsequently a valence d electron with spin $-\sigma$ can fill the core-hole and an outgoing x-ray is emitted. The net result of this RIXS process is a spin-flip transition $\sigma \rightarrow -\sigma$ in the TM d-shell, which is the same as the net result of inelastic neutron scattering involving this d-shell electron.

When a K-edge is used instead of a L-edge, this direct spin-flip process is no longer allowed. This is because in K-edge RIXS an electron is excited from a core-shell with s-symmetry, for which spin-orbit coupling is simply absent. It thus appears that for RIXS at K-edges direct spin-flip scattering is forbidden and only higher order magnetic scattering processes – starting at double spin-flip (e.g. bi-magnon) scattering – are allowed [17–19]. Indeed bi-magnon scattering is observed both at TM [20, 21] and oxygen (O) K-edges [22, 23]. This apparent absence of single-magnon spin-flip scattering is unfortunate because the O K-edge is in a soft x-ray regime where the RIXS resolution is particularly high (even if in this situation only a limited part of momentum space is accessible) and oxygen anions are obviously ubiquitous in magnetic materials.

However, in this Letter we show that single-magnon (SM) scattering at O K-edges is allowed when spin-orbit coupling is present in the TM d-shell *and* inversion symmetry at the O-site is broken. Our symmetry analysis and exact diagonalization study shows that the resulting SM-scattering is allowed for small momentum losses and forbidden for momenta close to the magnetic ordering vector, a situation opposite to magnetic RIXS at the TM L-edge. As in iridates the spin-orbit interaction in the $5d$ shell is large and the inversion symmetry at O-sites is often distinctly broken, as e.g. in the perovskites Sr_2IrO_4, $Sr_3Ir_2O_7$, Na_2IrO_3 and the post-perovskite $CaIrO_3$, we predict pronounced SM-scattering at the O K-edge of for instance these magnetic oxides.

RIXS cross section — When an incident (outgoing) x-ray with ϵ (ϵ') polarization has the frequency $\omega_{\mathbf{k}}$ ($\omega_{\mathbf{k}'}$) and wave vector $\mathbf{k}$ ($\mathbf{k}'$), the RIXS intensity is described by the Kramers-Heisenberg relation [4]

$$I(\omega, \mathbf{q}, \epsilon, \epsilon') = \sum_f |\mathcal{F}_{fg}(\omega, \mathbf{q}, \epsilon, \epsilon')|^2 \times \delta\left(E_f + \hbar\omega_{\mathbf{k}} - E_g - \hbar\omega_{\mathbf{k}'}\right), \quad (1)$$

where, $\omega = \omega_{\mathbf{k}} - \omega_{\mathbf{k}'}$ and $\mathbf{q} = \mathbf{k} - \mathbf{k}'$. In the dipole and fast collision approximation, the scattering amplitude $\mathcal{F}_{fg}$ is reduced to $\mathcal{F}_{fg} = \frac{1}{i\Gamma}\langle f|R(\epsilon', \epsilon, \mathbf{q})|g\rangle$, where R is the effective RIXS scattering operator, which is defined by the product of two dipole operators, and Γ is the core-hole broadening [4]. When ψ_ν and ψ_s represent valence and core states, the scattering operator is given by

$$R(\epsilon', \epsilon, \mathbf{q}) = \sum_{i\nu\nu'} e^{i\mathbf{q}\cdot\mathbf{r}_i} T_{\nu'\nu}(\epsilon', \epsilon) c_{i\nu'} c^\dagger_{i\nu}, \quad (2)$$

where $T_{\nu'\nu}(\epsilon', \epsilon) = \sum_s \langle\psi_{\nu'}|\epsilon'\cdot\mathbf{r}|\psi_s\rangle\langle\psi_s|\epsilon\cdot\mathbf{r}|\psi_\nu\rangle$. In case of the O K-edge RIXS, $T_{\nu'\nu}(\epsilon', \epsilon)$ equals $\frac{1}{3}\epsilon_{m'}\epsilon_m\delta_{\sigma',\sigma}\langle r\rangle^2$

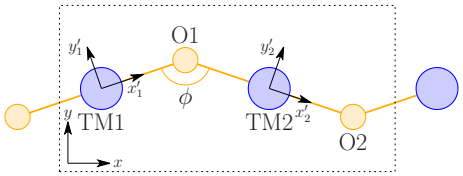

FIG. 1: (Color online) Schematic diagram of corner-sharing TM-O system, which for bond-angle ϕ not equal to 180° lacks inversion symmetry at the oxygen site. The z-direction is out of plane.

where ν has m (x, y, or z) orbital and σ spin characters. The most important feature of the O K-edge RIXS process is that in its intermediate state, besides an oxygen core-hole, also an extra valence electron is present the system that hybridizes and interacts with the TM d-electrons.

Symmetry analysis — To investigate the magnetic response of the O K-edge RIXS, we start by considering a simple TM1-O1-TM2-O2 arrangement of transition metal and oxygen ions, where the TM-O-TM bond angle is ϕ, see Fig. 1. To be specific, we concentrate on iridates (cuprates) in the following symmetry analysis, in which the Ir^{4+} (Cu^{2+}) ions are in a $5d^5$ ($3d^9$) configuration. Due to the strong spin-orbit coupling, Ir^{4+} ions in iridate form effective $J_{eff} = 1/2$ moments [24, 25] so that the single-site ground-state multiplet is a Kramers doublet, which we denote by D. Also in the case of Cu^{2+} in cuprates, a Kramers doublet ($S = 1/2$) is the ground state as the tetragonal crystal field splits up the e_g orbital degeneracy. When one considers two of these moments, the magnetic interactions between them cause a splitting into a total singlet (S) and a total triplet (T) state. The four states are $|S\rangle = \frac{1}{2}\left(|D_\uparrow D_\downarrow; 00\rangle - |D_\downarrow D_\uparrow; 00\rangle\right)$, $|T_1\rangle = |D_\uparrow D_\uparrow; 00\rangle$, $|T_0\rangle = \frac{1}{2}\left(|D_\uparrow D_\downarrow; 00\rangle + |D_\downarrow D_\uparrow; 00\rangle\right)$, and $|T_{-1}\rangle = |D_\downarrow D_\downarrow; 00\rangle$, where $|00\rangle$ denotes the *absence of holes* on the oxygen sites, in the O p-orbitals. Because of the hopping t_{pd} between TM and O, such charge-transfer states of course mix in. We denote such a charge-transfer state with a hole on oxygen as $|D_\sigma A; \xi 0\rangle$, where A represents the Ir $5d^6$ (Cu $3d^{10}$) state, in which all doublet states are occupied, and ξ refers to the p-hole state of O.

We now introduce two different inversion symmetry operators $I_{\rm O}$ and I_{TM} that represent inversion with respect to O and TM centers, respectively. When $I_{\rm O}$ and I_{TM} are applied, local coordinates transform as $I_{\rm O}: \ (x_1', y_1') \to (-x_2', -y_2'), (x_1, y_1) \to (-x_1, -y_1)$ and $I_{TM}: \ (x_1', y_1') \to (-x_1', -y_1'), (x_1, y_1) \to (-x_2, -y_2)$. We note that I_{TM} is *always* a symmetry of the system, but $I_{\rm O}$ is a symmetry operator *only for* $\phi = 180°$, i.e. undistorted TM-O-TM bonds. Because of I_{TM} symmetry, the hopping integrals between singlet/triplet and charge-transfer states obey the relations $\langle S|H_t|D_\sigma A; \xi 0\rangle = -\langle S|H_t|D_\sigma A; 0\xi\rangle$ and $\langle T_m|H_t|D_\sigma A; \xi 0\rangle = -\langle T_m|H_t|D_\sigma A; 0\xi\rangle$, where H_t is the TM-O hopping part of the Hamiltonian, so that the singlet ground state $|g\rangle$ and triplet excites states $|m\rangle$ become

$$|g\rangle = c|S\rangle + \sum_{\sigma\xi} c_{\sigma\xi}\big(|D_\sigma A; \xi 0\rangle - |D_\sigma A; 0\xi\rangle\big) + \cdots,$$

$$|m\rangle = c_m|T_m\rangle + \sum_{\sigma\xi} c_{m\sigma\xi}\big(|D_\sigma A; \xi 0\rangle - |D_\sigma A; 0\xi\rangle\big) + \cdots,$$

which directly follows from the symmetry properties of the states involved given explicitly in Table I.

TABLE I: Transformation properties of singlet ($|S\rangle$), triplet ($|T\rangle$), and charge transfer ($|D_\sigma A; \xi 0\rangle$) states under two types of inversion, $I_{\rm O}$ and I_{TM}. Note that $I_{\rm O}$ is only a symmetry when the bond angle $\phi = 180°$.

	$\lvert S\rangle$	$\lvert T\rangle$	$\lvert D_\sigma A; \xi 0\rangle$
$I_{\rm O}(\phi = 180°)$	$-\lvert S\rangle$	$\lvert T\rangle$	$-\lvert AD_\sigma; \xi 0\rangle$
I_M	$\lvert S\rangle$	$\lvert T\rangle$	$-\lvert DA_\sigma; 0\xi\rangle$

Next we require the symmetry properties of the effective RIXS scattering operator $R(\epsilon', \epsilon, \mathbf{q})$ in Eq. (2) under inversion. These explicitly depend on the momentum $\mathbf{q}$ that is transferred by a x-ray photon to the system: only for momenta corresponding to high symmetry points in the Brillouin Zone (BZ), a symmetry analysis is viable, in the present case in particular for $q = 0$ and $q = \pi$. For these momenta the transformation properties of R under the two types of inversion, $I_{\rm O}$ and I_{TM}, are summarized in Table II, considering both RIXS at the O K-edge and the Ir L_3-edge.

Having determined these transformation properties, it can immediately verified that the RIXS scattering amplitude $\mathcal{F}_{mg}^{OK}$ at the O K-edge between ground state $|g\rangle$ and magnetically excited state $|m\rangle$ obeys the selection rule $\mathcal{F}_{mg}^{OK}(q = \pi) = 0$ for all m, because $I_{TM}^\dagger R(q = \pi) I_{TM} = -R$. For $q = 0$ no such selection rule is dictated by I_{TM}. However, in the situation that the bond-angle is 180° and $I_{\rm O}$ is a symmetry of the system, the relations $\langle S|H_t|D_\sigma A; \xi 0\rangle = \langle S|H_t|AD_\sigma; \xi 0\rangle$ and $\langle T_m|H_t|D_\sigma A; \xi 0\rangle = -\langle T_m|H_t|AD_\sigma A; \xi 0\rangle$ hold, which imply that in addition $\mathcal{F}_{mg}^{OK}(q = 0) = 0$. Conversely, this implies that magnetic scattering at the O K-edge is *allowed* at $q = 0$ and its vicinity when $\phi \neq 180^o$ and inversion symmetry at the O-site is broken.

TABLE II: Symmetry properties of RIXS scattering operator R at the O K-edge and Ir L_3-edge with respect to two types of inversions, $I_{\rm O}$ and I_{TM}.

	Ir L-edge		O K-edge	
	$q = 0$	$q = \pi$	$q = 0$	$q = \pi$
$I_{\rm O}(\phi = 180°)$	R	$-R$	R	R
I_{TM}	R	R	R	$-R$

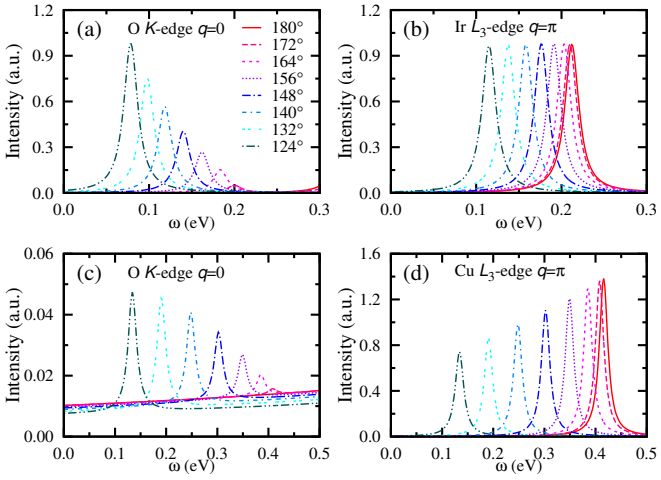

FIG. 2: (Color online) Magnetic RIXS spectra calculated by ED as a function of TM-O-TM bond angle ϕ. (a) Iridate O K-edge at $q = 0$, (b) Ir L_3-edge at $q = \pi$, (c) Cuprate O K-edge RIXS at $q = 0$, (d) Cu L_3-edge at $q = \pi$. The polarizations are $\epsilon = x$ and $\epsilon' = z$. Note that as a function of ϕ both the effective magnetic interactions and the RIXS intensity change.

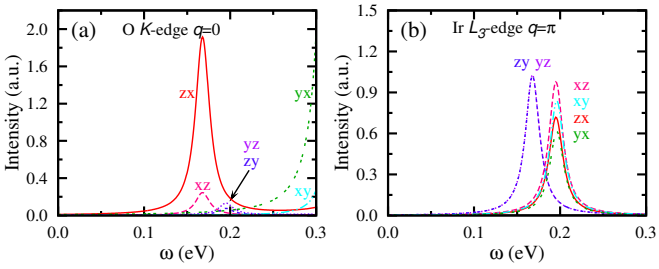

FIG. 3: (Color online) Polarization dependence of magnetic RIXS excitations for an iridate cluster with an Ir-O-Ir bond-angle of $\phi = 158°$. (a) O K-edge at $q = 0$, (b) Ir L_3-edge at $q = \pi$. The polarization condition zx labels $\epsilon = z$, $\epsilon' = x$.

It is interesting to perform an analogue symmetry analysis for magnetic RIXS at the L-edge RIXS. The scattering amplitude $\mathcal{F}^L_{mg}$ is proportional to $c^* c_m \langle T_m|R|S\rangle$ and it can easily be verified that I_{TM} does not give rise to any selection because both $|S\rangle$ and $|T_m\rangle$ have the same parity under I_{TM}. Interestingly, for straight bonds with $\phi = 180°$, where $I_{\rm O}$ is a symmetry of the system, $\mathcal{F}^L_{mg}(q = 0) = 0$. This is related to the fact that for $I_{\rm O}$ the singlet and triplet states have different parities. These selection rules are of course directly related to the experimental and theoretical observations that on iridates and cupartes the magnetic L-edge RIXS intensity peaks at the edge of the BZ [2, 3, 10–12].

Exact diagonalization results — In order to test these symmetry-based selection rules and to determine in addition their dependence in the incoming and outgoing polarization of x-ray photons, we perform an exact diagonalization study of the relevant microscopic model Hamiltonian for iridates and cuprates on small clusters. The generic Hamiltonian is $H = \sum_{ij} H_i^{\rm TM} + H_j^{\rm O} + H_{ij}^t$, where $H_i^{\rm TM}$ and $H_j^{\rm O}$ refer to the local Hamiltonian of TM and O ions on neighboring sites i and j and H_{ij}^t captures the hopping of electrons on the connecting TM-O bond [26]. Further details are provided in the supplementary material.

The RIXS spectra, calculated as a function of the TM-O bond angle ϕ are shown in Fig. 2, where the two top panels are the results for an Ir^{4+} cluster and the two lower panels are for a Cu^{2+} cluster, with on the left the magnetic scattering at the oxygen K-edges and on the right RIXS intensities at the TM L-edges [27]. There are many charge excitations at higher energy, but we focus on only the low-energy, magnetic part of the excitation spectra. The overall trends are very similar. First of all, it is clear that when ϕ starts to deviate from 180°, the energy of the magnetic excitations goes down, which is due to the reduction of the effective exchange interaction between the (iso)spins, as the hopping integrals directly depend on the bond-angle. This is equally true for RIXS at the Ir or Cu L-edges and at the corresponding O K-edges. A big difference is, however, that for straight bonds, where $\phi = 180°$, the O K-edge magnetic scattering intensity vanishes, whereas the TM L-edge intensity is finite in both cases. This is the result of the selection rules derived above. Only when the bond-angle ϕ begins to deviate from 180°, magnetic RIXS intensity starts to build up at the O K-edge. It should be noted, however, that for typical parametrizations of quasi-2D perovskite iridates and cuprates, the magnetic scattering intensity at the oxygen edge is at least ~ 20 times larger in the irradiate compared to the cuprate. This reflects the fact that the spin-orbit coupling in iridates is much larger.

It is interesting to analyze the polarization dependence of the RIXS amplitude for an iridate with buckled bonds. The polarization direction of the incoming (ϵ) and outgoing (ϵ') x-ray are defined in the coordinate system of Fig. 1 and the resulting RIXS spectra shown in Fig. 3. It should first of all be noted that there are two sets of magnetic excitations because of the additional anisotropic interactions (Dzyaloshinskii-Moriya and Kitaev exchange terms) that are generated by the buckling of bonds [28, 29], splitting up the excited magnetic states. At the Ir L-edge, one set of magnetic modes is picked up in yz and zy polarization, and the other four orthogonal polarization conditions pick up the other magnetic mode. The magnetic scattering is only present in cross-polarization conditions, which reflects the fact that in SM scattering angular momentum is transferred from the x-ray photon to the magnon. This is also reflected in the O K-edge, RIXS, where depending on the specific polarization conditions, either of the magnetic modes is picked up (zx, xz versus yz, zy), or none (yx and xy). Note that the magnetic scattering intensity is by far largest for the

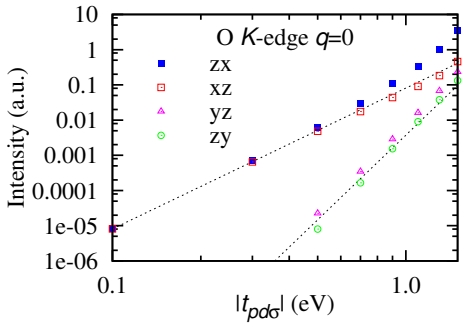

FIG. 4: (Color online) Magnetic RIXS intensity at the O K-edge as a function of the Ir-O hopping $t_{pd\sigma}$ on a log-log scale, for fixed $\phi = 158°$. The two dotted lines represent proportionalities to $t^4_{pd\sigma}$ and $t^8_{pd\sigma}$.

situation of incoming polarization in the z-direction and outgoing polarization along the x-axis. Note that in the spectra we do not show the elastic contribution to the resonant scattering, which in principle produces a zero-loss peak.

It is clear that the calculated magnetic RIXS intensity at the oxygen K-edge of iridates, apart from symmetry, critically depends on an interplay of the spin-orbit coupling and the hybridization between oxygen p and iridium d states – without either one or the other the magnetic RIXS intensity vanishes. In the cluster the Ir-O hopping is parametrized by $t_{pd\sigma}$ and the magnetic scattering intensity as a function of $t_{pd\sigma}$ is shown in Fig. 4 on a log-log scale for a fixed bond-angle of 158°. It makes clear that there are two types of contributions to the intensity, scaling with $t^4_{pd\sigma}$ and $t^8_{pd\sigma}$, respectively, in the weak hopping limit. Moreover, which contribution is picked up strongly depends on polarization conditions of the experiment. This is of course very different from magnetic RIXS intensities at transition metal L-edges and their polarization dependence, which are in leading order finite and independent of $t_{pd\sigma}$.

Summary and conclusions — We have shown on the basis of a symmetry analysis and exact diagonalization study, that magnon scattering at O K-edges becomes allowed when the inversion symmetry at the O-site is broken, for instance by a buckling of bonds. For cuprates the resulting magnetic RIXS intensity is tiny but iridates may have the spin-orbit energy scale that is needed and also can fulfill the symmetry requirements. The first type of material that may come to mind to observe single-magnon modes with oxygen K-edge RIXS, are the quasi-2D iridates as Sr_2IrO_4 and Ba_2IrO_4, in which L-edge RIXS has already established the presence of distinct magnon modes [10]. One can easily extent our symmetric analysis to the corresponding 2D lattices, which are still invariant under I_{TM} and break I_O when the IrO_4 octahedra buckle. But even if the spin-orbit coupling and the Ir-O hybridization $t_{pd\sigma}$ are significant in these materials, the Ir-O-Ir buckling angle for these systems is rather small, or even vanishing [30]. A better candidate system is the post-perovskite $CaIrO_3$ in which a strong antiferromagnetic interaction along the c axis (J_c) is present, where at the same time the corner-sharing octahedra are significantly buckled. Along the a axis the octahedra are edge-sharing, which leads to weak ferromagnetic interactions so that magnetically $CaIrO_3$ is a quasi-one-dimensional system [31, 32], with $|J_c/J_a| >> 1$ – it thereby becomes an ideal candidate to observe single-magnon RIXS at the oxygen K-edge.

Acknowledgements — We thank Thorsten Schmitt and Giniyat Khaliullin for fruitful discussions. B.H.K was supported by the Basic Science Research Program through the National Research Foundation of Korea (NRF) funded by the Ministry of Education, Science and Technology (2013R1A6A3A0302053).

[1] L. J. P. Ament, G. Ghiringhelli, M. Moretti Sala, L. Braicovich, and J. van den Brink, Phys. Rev. Lett. **103**, 117003 (2009).
[2] L. Braicovich, L. J. P. Ament, V. Bisogni, F. Forte, C. Aruta, G. Balestrino, N. B. Brookes, G. M. De Luca, P. G. Medaglia, F. M. Granozio, et al., Phys. Rev. Lett. **102**, 167401 (2009).
[3] L. Braicovich, J. van den Brink, V. Bisogni, M. Moretti Sala, L. J. P. Ament, N. B. Brookes, G. M. De Luca, M. Salluzzo, T. Schmitt, V. N. Strocov, et al., Phys. Rev. Lett. **104**, 077002 (2010).
[4] L. J. P. Ament, M. van Veenendaal, T. P. Devereaux, J. P. Hill, and J. van den Brink, Rev. Mod. Phys. **38**, 705 (2011).
[5] M. Le Tacon, G. Ghiringhelli, J. Chaloupka, M. Moretti Sala, V. Hinkov, M. W. Haverkort, M. Minola, M. Bakr, K. J. Zhou, S. Blanco-Canosa, et al., Nature Physics **7**, 725 (2011).
[6] M. Le Tacon, M. Minola, D. C. Peets, M. Moretti Sala, S. Blanco-Canosa, V. Hinkov, R. Liang, D. A. Bonn, W. N. Hardy, C. T. Lin, et al., Phys. Rev. B **88**, 020501(R) (2013).
[7] M. P. M. Dean, A. J. A. James, R. S. Springell, X. Liu, C. Monney, K. J. Zhou, R. M. Konik, J. S. Wen, Z. J. Xu, G. D. Gu, et al., Phys. Rev. Lett. **110**, 147001 (2013).
[8] M. P. M. Dean, G. Dellea, R. S. Springell, F. Yakhou-Harris, N. B. Kummer, K. Brookes, X. Liu, Y.-J. Sun, J. Strle, T. Schmitt, L. Braicovich, et al., Nature Materials **12**, 1019 (2013).
[9] L. J. P. Ament, G. Khaliullin, and J. van den Brink, Phys. Rev. B **84**, 020403(R) (2011).
[10] J. Kim, D. Casa, M. H. Upton, T. Gog, Y.-J. Kim, J. F. Mitchell, van Veenendaal M., M. Daghofer, J. van den Brink, G. Khaliullin, et al., Phys. Rev. Lett. **108**, 177003 (2012).
[11] J. Kim, A. H. Said, D. Casa, M. H. Upton, T. Gog, M. Daghofer, G. Jackeli, J. van den Brink, G. Khaliullin, and B. J. Kim, Phys. Rev. Lett. **109**, 157402 (2012).
[12] H. Gretarsson, J. P. Clancy, Y. Singh, P. Gegenwart, J. P. Hill, J. Kim, M. H. Upton, A. H. Said, D. Casa, T. Gog,

et al., Phys. Rev. B **87**, 220407(R) (2013).
[13] M. W. Haverkort, Phys. Rev. Lett. **105**, 167404 (2010).
[14] M. van Veenendaal (2011), arXiv:1106.0640.
[15] J.-i. Igarashi and T. Nagao, Phys. Rev. B **88**, 014407 (2013).
[16] J.-i. Igarashi and T. Nagao, Phys. Rev. B **89**, 064410 (2014).
[17] J. van den Brink, Europhys. Lett. **80**, 47003 (2007).
[18] T. Nagao and J.-i. Igarashi, Phys. Rev. B **75**, 214414 (2007).
[19] F. Forte, L. J. P. Ament, and J. van den Brink, Phys. Rev. B **77**, 134428 (2008).
[20] J. P. Hill, G. Blumberg, Y.-J. Kim, D. S. Ellis, S. Wakimoto, R. J. Birgeneau, S. Komiya, Y. Ando, B. Liang, R. L. Greene, et al., Phys. Rev. Lett. **100**, 097001 (2008).
[21] D. S. Ellis, J. Kim, J. P. Hill, S. Wakimoto, R. J. Birgeneau, Y. Shvyd'ko, D. Casa, T. Gog, K. Ishii, K. Ikeuchi, et al., Phys. Rev. B **81**, 085124 (2010).
[22] V. Bisogni, L. Simonelli, L. J. P. Ament, F. Forte, M. Moretti Sala, M. Minola, H. S., J. van den Brink, G. Ghiringhelli, N. B. Brookes, et al., Phys. Rev. B **85**, 214527 (2012).
[23] V. Bisogni, M. Moretti Sala, A. Bendounan, N. B. Brookes, G. Ghiringhelli, and L. Braicovich, Phys. Rev. B **85**, 214528 (2012).
[24] B. J. Kim, H. Jin, S. J. Moon, J.-Y. Kim, B.-G. Park, C. S. Leem, J. Yu, T. W. Noh, C. Kim, S.-J. Oh, et al., Phys. Rev. Lett. **101**, 076402 (2008).
[25] B. J. Kim, H. Ohsumi, T. Komesu, S. Sakai, T. Morita, H. Takagi, and T. Arima, Science **323**, 1329 (2009).
[26] See the supplementary material for the detail of Hamiltonians and parametrizations of clusters with formally either Ir^{4+} or Cu^{2+} ions, and numerical method.
[27] As symmetry analysis, our calculation yields no single-magnon peak in the O K-edge RIXS spectra at $q = \pi$. The magnetic peak, however, is observed in the TM L-edge at $q = 0$. See the supplementary material for its detail.
[28] G. Jackeli and G. Khaliullin, Phys. Rev. Lett. **102**, 017205 (2009).
[29] B. H. Kim, G. Khaliullin, and B. I. Min, Phys. Rev. Lett. **109**, 167205 (2012).
[30] M. Moretti Sala, M. Rossi, S. Boseggia, J. Akimitsu, N. B. Brookes, M. Isobe, M. Minola, H. Okabe, H. M. Rønnow, L. Simonelli, et al., Phys. Rev. B **89**, 121101(R) (2014).
[31] N. A. Bogdanov, V. M. Katukuri, H. Stoll, J. van den Brink, and L. Hozoi, Phys. Rev. B **85**, 235147 (2012).
[32] K. Ohgushi, J.-i. Yamaura, H. Ohsumi, K. Sugimoto, S. Takeshita, A. Tokuda, H. Takai, M. Takata, and T.-h. Arima, Phys. Rev. Lett. **110**, 217212 (2013).

Supplemental Material: Resonant inelastic x-ray scattering on single-magnons at oxygen K-edges

MICROSCOPIC HAMILTONIAN AND NUMERICAL METHOD

To investigate the magnetic response of the oxygen (O) K- and transition-metal (TM) L-edge resonant inelastic x-ray scattering (RIXS) spectra of iridates and cuprates, we considered the periodic TM1-O1-TM2-O2 cluster (see Fig. 1) which is described by following Hamiltonian:

$$H = \sum_{ij} H_i^{\mathrm{TM}} + H_j^{\mathrm{O}} + H_{ij}^t, \tag{3}$$

where H_i^{TM} and H_j^{O} refer to local energy of i-th TM and j-th O ions, respectively, and H_{ij}^t represents the hopping Hamiltonian between neighboring TM-O bonds. The local Hamiltonians of TM and O sites are as follows.

$$H^{\mathrm{TM}} = \sum_{\mu\sigma} \epsilon_\mu n_{\mu\sigma} + \lambda \sum_{\mu\nu\sigma\sigma'} (\mathbf{l}\cdot\mathbf{s})_{\mu\sigma,\nu\sigma'} c^\dagger_{\mu\sigma} c_{\nu\sigma'} + \frac{1}{2}\sum_{\sigma\sigma'\mu\nu} U_{\mu\nu} c^\dagger_{\mu\sigma} c^\dagger_{\nu\sigma'} c_{\nu\sigma'} c_{\mu\sigma} + \frac{1}{2}\sum_{\substack{\sigma\sigma'\\ \mu\neq\nu}} J_{\mu\nu} c^\dagger_{\mu\sigma} c^\dagger_{\nu\sigma'} c_{\mu\sigma'} c_{\nu\sigma}$$
$$+\frac{1}{2}\sum_{\substack{\sigma\\ \mu\neq\nu}} J'_{\mu\nu} c^\dagger_{\mu\sigma} c^\dagger_{\mu\bar{\sigma}} c_{\nu\bar{\sigma}} c_{\nu\sigma}, \tag{4}$$

where $U_{\mu\mu} = U$, $U_{\mu\neq\nu} = U - 2J_H$, and $J_{\mu\nu} = J'_{\mu\nu} = J_H$. $\bar{\sigma}$ stands for the opposite sign of σ. We set ϵ_μ so that $-1/3\Delta_t$ for yz and zx, $2/3\Delta_t$ for xy, $10Dq - 3/2\Delta_t$ for z^2, and $10Dq + 3/2\Delta_t$ for $x^2 - y^2$.

$$H^{\mathrm{O}} = \epsilon_p \sum_{m\sigma} n_{m\sigma} + \frac{1}{2}\sum_{\sigma\sigma' mn} U_{mn} c^\dagger_{m\sigma} c^\dagger_{n\sigma'} c_{n\sigma'} c_{m\sigma} + \frac{1}{2}\sum_{\substack{\sigma\sigma'\\ m\neq n}} J_{mn} c^\dagger_{m\sigma} c^\dagger_{n\sigma'} c_{m\sigma'} c_{n\sigma} + \frac{1}{2}\sum_{\substack{\sigma\\ m\neq n}} J'_{mn} c^\dagger_{m\sigma} c^\dagger_{m\bar{\sigma}} c_{n\bar{\sigma}} c_{n\sigma}, \tag{5}$$

where $U_{mm} = U_p$, $U_{m\neq n} = U_p - 2J_p$, and $J_{mn} = J'_{mn} = J_p$. ϵ_p is determined for the charge transfer energy (Δ) to be the minimum energy between d^5p^6 (d^9p^6) and d^6p^5 ($d^{10}p^5$) configurations for iridates (cuprates). Hopping Hamiltonian is given by

$$H_{ij}^t = \sum_{\mu m\sigma} \left(t^{ij}_{\mu m} c^\dagger_{jm\sigma} c_{i\mu\sigma} + h.c. \right), \tag{6}$$

where $t^{ij}_{\mu m}$ is a function of two parameters $t_{pd\sigma}$ and $t_{pd\pi}$ based on the Slater-Koster theory [S1].

We restricted the Hilbert space in order to include all possible states whose configuration is d^n-d^n-p^6-p^6, d^{n-1}-d^{n+1}-p^6-p^6, d^n-d^{n+1}-p^5-p^6, d^{n+1}-d^{n+1}-p^5-p^5, or d^{n+1}-d^{n+1}-p^4-p^6 where $n = 5$ ($n = 9$) for iridate (cuprate). We took into account the following relevant local multiplets to describe electronic states of Ir (Cu) ions: 6 (4) lowest multiplets for d^5 (d^9), 14 (6) lowest multiplets for d^4 (d^8), and 1 (1) lowest mutliplets for d^6 (d^{10}). Because only t_{2g}-hole (e_g-hole) states play a dominant role in low energy excitations of iridates (cuprates), they are enough to describe the single-magnon contribution in the RIXS spectra [S2, S3]. We constructed the Hilbert space so that each state can be expressed as the direct product of local multiplets of TM and O ions.

We adopted physical parameters as shown in table S1 (table S2) for iridates (cuprates) and solved the Hamiltonian by using the exact diagonalization. We calculated the RIXS spectra as following Kubo formula:

$$I = \frac{1}{\Lambda^2}\sum_n |\langle n|R|g\rangle|^2 \delta(\omega - E_n + E_g) \tag{7}$$

where E_g (E_n) is the energy of the ground state $|g\rangle$ (the excited state $|n\rangle$) and R is the RIXS scattering operator.

TABLE S1: Physical parameters for iridates in units of eV, consistent with previous work [S2].

$10Dq$	Δ_t	U	J_H	λ	Δ	U_p	J_p	$t_{pd\sigma}$	$t_{pd\pi}$
3.0	0.10	1.86	0.50	0.4	3.3	0.5	0.1	-1.5	$-0.46t_{dp\sigma}$

TABLE S2: Physical parameters for cuprates in units of eV, consistent with previous work [S4].

$10Dq$	Δ_t	U	J_H	λ	Δ	U_p	J_p	$t_{pd\sigma}$	$t_{pd\pi}$
1.5	−0.10	8.0	0.5	0.1	2.5	0.5	0.1	−1.0	$-0.46t_{dp\sigma}$

RIXS SPECTRA FOR IRIDIUM L-EDGE RIXS AT $q = 0$

As shown in table II, the RIXS scattering operator of the Ir L-edge at $q = 0$ has same symmetric property as that of the O K-edge. It can be also expected for the Ir L-edge RIXS to give rise to the magnetic peak at $q = 0$. Accordingly our numerical calculation yields nonzero magnetic RIXS peak of the Ir L-edge at $q = 0$. Figure S1 presents the magnetic RIXS peak of the L_3-edge at $q = 0$ with respect to bond angle and x-ray polarization. Overall features are totally same as those in the O K-edge (see Fig. 2(a) and 3(a)). The magnetic peak at $q = 0$ is only allowed when the Ir-O-Ir bond is buckled. The magnetic modes is dominantly picked up at zx and xz polarizations. Neither yx, nor xy, nor xx polarization gives any magnetic peak. Thus the broken inversion with oxygen center can induce the magnetic excitation at center of the BZ even though its intensity is much more suppressed than that at the edge.

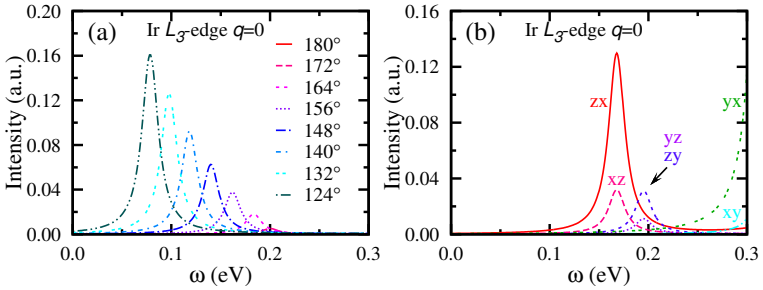

FIG. S1: (Color online) Magnetic RIXS spectra of the Ir L_3-edge at $q = 0$ as a function of (a) Ir-O-Ir bond angle and (b) x-ray polarization. $\phi = 158^\circ$ is set in (b).

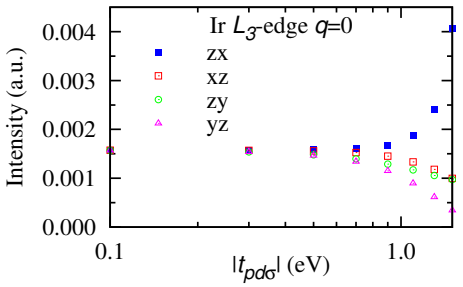

FIG. S2: (Color online) Magnetic RIXS intensity of the Ir L_3-edge at $q = 0$ as a function of the Ir-O hopping for fixed $\phi = 158^\circ$.

The L-edge RIXS process, however, is not directly related to O states. For this reason, the magnetic RIXS intensity at the Ir L-edge is almost independent with the Ir-O hopping strength in contrast with the O K-edge, of which intensity is proportional to $t^4_{pd\sigma}$ or $t^8_{pd\sigma}$. Figure S2 describes this feature well. In weak hopping limit, total magnetic RIXS intensity is almost constant. In strong hopping limit, of course, even Ir L-edge is remarkably affected due to considerable overlap between local Ir multiplet states and charge-transfer states.

[S1] J. C. Slater and G. F. Koster, Phys. Rev. **94**, 1498 (1954).
[S2] B. H. Kim, G. Khaliullin, and B. I. Min, Phys. Rev. Lett. **109**, 167205 (2012)
[S3] B. H. Kim, G. Khaliullin, and B. I. Min, Phys. Rev. B **89**, 081109(R) (2014)
[S4] M. Imada, A. Fujimori, and Y. Tokura, Rev. Mod. Phys. **70**, 1039 (1998).